Bzdrenga et al. BMC Research Notes 2014, 7:333
http://www.biomedcentral.com/1756-0500/7/333

BMC Research Notes

RESEARCH ARTICLE Open Access

*Sac*Pox from the thermoacidophilic crenarchaeon *Sulfolobus acidocaldarius* is a proficient lactonase

Janek Bzdrenga[1†], Julien Hiblot[1†], Guillaume Gotthard[1], Charlotte Champion[1], Mikael Elias[2*] and Eric Chabriere[1*]

Abstract

Background: *Sac*Pox, an enzyme from the extremophilic crenarchaeal *Sulfolobus acidocaldarius* (*Sac*), was isolated by virtue of its phosphotriesterase (or paraoxonase; Pox) activity, *i.e.* its ability to hydrolyze the neurotoxic organophosphorus insecticides. Later on, *Sac*Pox was shown to belong to the Phosphotriesterase-Like Lactonase family that comprises natural lactonases, possibly involved in *quorum* sensing, and endowed with promiscuous, phosphotriesterase activity.

Results: Here, we present a comprehensive and broad enzymatic characterization of the natural lactonase and promiscuous organophosphorus hydrolase activities of *Sac*Pox, as well as a structural analysis using a model.

Conclusion: Kinetic experiments show that *Sac*Pox is a proficient lactonase, including at room temperature. Moreover, we discuss the observed differences in substrate specificity between *Sac*Pox and its closest homologues *Sso*Pox and *Sis*Lac together with the possible structural causes for these observations.

Keywords: Lactonase, PLL, *Quorum* sensing, Phosphotriesterase, Extremophile, Thermoacidophile

Background

Phosphotriesterase-Like Lactonases (PLLs) are natural lactonases (EC 3.1.1.25) (Figure 1C, D, E) with promiscuous phosphotriesterase activity (EC 3.1.8.1) (Figure 1A) [1,2]. They are structurally closely related to bacterial phosphotriesterases (PTEs) [3-6], such as *Brevundimonas diminuta* PTE (*Bd*PTE; ~30% sequence identity) [7]. PTEs naturally hydrolyze neurotoxic organophosphorus (OPs) compounds (Figure 1A) such as paraoxon (the active metabolite of the insecticide parathion) with catalytic constants that approach the diffusion limit (*i.e.* $k_{cat}/K_M \sim 10^8\ M^{-1}\ s^{-1}$) [7]. Because OPs have been massively used as pesticides since the 50's [8], PTEs are believed to have emerged in few decades from a PLL progenitor [2], providing a new source of phosphorus to bacteria, and consequently a selective advantage [8].

Both enzyme families exhibit the same $(\beta/\alpha)_8$-barrel topology [9,10] and belong to the amidohydrolase superfamily [11,12]. Their structure consists of 8 β-strands forming a central barrel surrounded by 8 α-helixes. The active site is constituted by a bimetallic center (two metal cations) localized at the C-terminus of the barrel. Metal cations are coordinated by four histidines, an aspartic acid and a carboxylated lysine residue [9]. While the nature of the bimetallic center can vary depending on the enzyme nature and the purification procedure [3,5,13,14], the catalytic mechanism is presumed to be identical. The bimetallic center activates a water molecule into a hydroxide ion which performs a nucleophilic attack onto the electrophilic center [9,15].

The difference in substrate specificities of PLLs and PTEs seems mainly governed by variation in the connecting loops of the barrel [2,16]. Major differences between PTEs and PLLs reside in the active site loop size and conformation [1,2]. Indeed, loop 7 is shorter in PLLs than in PTEs whereas the loop 8 is larger, forming a hydrophobic channel that accommodates lactones aliphatic chain [9]. Loop 7/8 length and sequence also differ within the PLL family and led to the identification of two different subfamilies: PLLs-A and PLLs-B [2]. Both subfamilies exhibit different substrate specificities: PLLs-B are exclusively oxo-lactonases (Figure 1DE) whereas PLLs-A hydrolyze efficiently oxo-lactones and Acyl-Homoserine Lactones (AHLs, Figure 1C) [2]. AHLs are messenger molecules involved in a bacterial communication system

* Correspondence: mikael.elias@gmx.fr; eric.chabriere@univ-amu.fr
†Equal contributors
[2]Weizmann Institute of Science, Biological Chemistry, Rehovot, Israel
[1]URMITE UMR CNRS-IRD 6236, IFR48, Faculté de Médecine et de Pharmacie, Université de la Méditerranée, Marseille, France

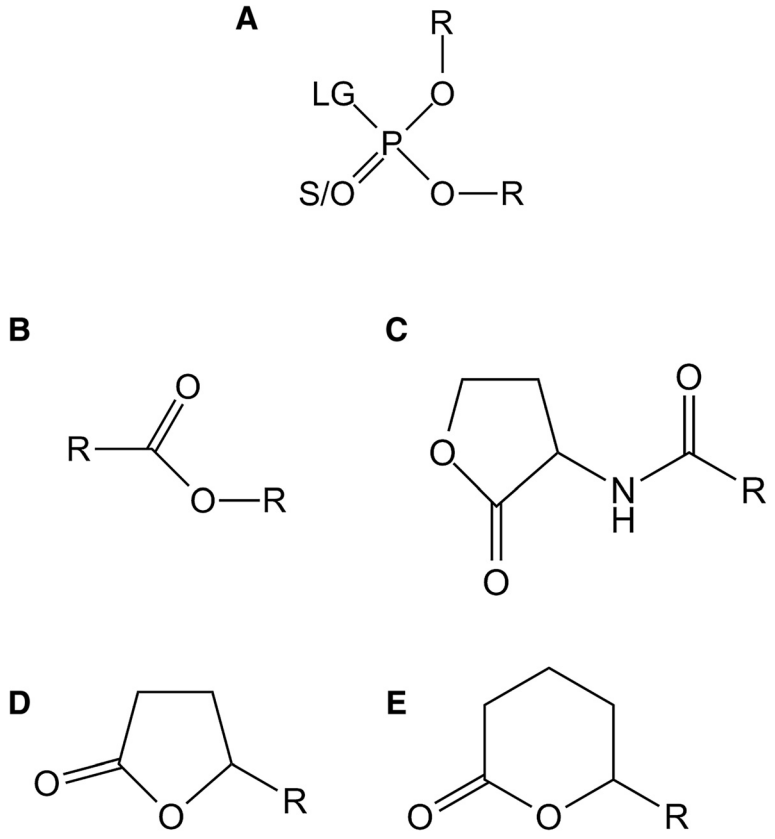

Figure 1 Chemical structure of *Sac*Pox substrates. Chemical structures of **(A)** phosphotriesters, **(B)** esters, **(C)** Acyl-Homoserine Lactones, **(D)** γ-lactones and **(E)** δ-lactones are presented. For phosphotriesters, R corresponds to different nature of substituents; LG corresponds to the leaving group. The terminal substituent could be S atom if the molecule is a thionophosphotriester or an O atom if the molecule is an oxonophosphotriester. For esters, R corresponds to different nature of substituent. For AHLs and γ/δ-lactones, R corresponds to different size of acyl chain.

dubbed *quorum* sensing (QS) [17]. QS regulates the expression of numerous genes, and enables bacterial population to adopt a "group" behavior, including the expression of virulence factors of some pathogens [18,19]. The involvement of PLLs-A in *quorum* sensing has not yet been demonstrated, and these enzymes are often found with no other AHL components, including in archaeal species [20]. However, the fact that they hydrolyze specifically the natural enantiomer of AHL indicates that it may be their native substrate [16].

PLLs are promiscuous enzymes that catalyze two chemical reactions of potential biotechnological interest. Indeed, the inhibition or "quenching" of the QS is seen as a possibly promising strategy to develop innovative therapies [21-25]. Indeed, lactonases such as PLLs can inhibit QS (known as *quorum* quenching, *i.e.* QQ) [26,27] and thereby annihilate the virulence of micro-organisms possessing an AHL-based QS system [28]. Moreover, PLLs are endowed with relatively low phosphotriesterase activity, but might be optimized against OPs and subsequently used for degrading organophosphorus pesticides [3,5,6,9,29] and nerve agents [30], for which no satisfactory remediation methods are currently available [31].

In addition, several PLLs members are thermostable [3,4,6,32-34]; *e.g.* PLLs from extremophilic crenarchaeaon sources [3,4,16,34]. These counterparts exhibit industry-compatible properties (*e.g.* thermal and detergent resistance) [35-37]; making them good starting point for *in vitro* improvement protocols [37,38]. Several studies report the engineering of thermostable PLLs and improvement of catalytic efficiency against OPs, including for *Sso*Pox [16,39], *Dr*OPH (*Deinococcus radiodurans* organophosphorus hydrolase) [6,40] and *Gk*L (*Geobacillus kaustropilus* lactonase) [41] but also for the lactonase activity of *Sso*Pox [16], MCP (*Mycobacterium avium* subsp. Paratuberculosis K-10 lactonase) [42] and *Gk*L [43].

Here we focus on *Sac*Pox, the PLL from the thermoacidophilic crenarchaeon *Sulfolobus acidocaldarius* (living conditions: 55–85°C, pH 2–3) [44]. *Sac*Pox was originally isolated and studied for its ability to hydrolyze OP compounds at high temperature [4]. The enzyme shares about 30% of sequence identity with *Bd*PTE and

about 70% with its closest homologues, *i.e. Sso*Pox from *Sulfolobus solfataricus* [3] and *Sis*Lac from *Sulfolobus islandicus* [33,45]. Being an enzyme from a hyperthermophile, *Sac*Pox is however less stable than *Sso*Pox (half-life of 5 min at 90°C [4] and of 4 h at 95°C [3,46], respectively). The kinetic characterizations performed on *Sac*Pox revealed that it hydrolyzes OP, ester and lactone molecules at high temperature [4,13]. However, only few substrates have been tested, and no natural lactones were assayed as substrate. In this study, we performed a broad kinetic characterization of *Sac*Pox at room temperature (25°C) for several OPs, esters (Figure 1B) and lactone molecules including AHLs, γ-lactones and δ-lactones in the aim to evaluate the biotechnological potentialities of this enzyme.

Methods

Sequence alignment

The sequence alignment was performed based on the previously published PLL sequence alignment [2], using the *T-coffee* server (expresso) [47,48] and manually improved with the *seaview* software [49]. It contains 29 different sequences (Additional file 1: Table S1). The sequence alignment was represented using the *BioEdit* 7.1.3 software [50]. Protein sequence identities were computed using *ClustalW* server [51]. The phylogenetic tree was performed using *PhyML* [49] and default parameters.

Protein production and purification

The protein production and subsequent purification steps were performed analogously to previously described [16,33,34,45,52-54]. In brief, the protein was heterologously produced in *Escherichia coli* strain BL21 (DE_3)-pGro7/GroEL (TaKaRa) at 37°C in ZYP medium [55]. When OD_{600nm} reaches 0.8, protein production was induced with addition of arabinose (0.2%, w/v) and $CoCl_2$ (2 mM) and temperature transition to 25°C for 20 hours. Cells were harvested by centrifugation, and pelleted cells were suspended in *lysis buffer* (50 mM HEPES pH 8, 150 mM NaCl, 0.2 mM $CoCl_2$, lysozyme 25 mg/ml, PMSF 0.1 mM, DNase I 10 mg/ml), stored at −80°C during 2 hours; then sonicated 3 times during 30 seconds (Branson Sonifier 450, 80% intensity and microtype limit of 8) and centrifuged. Taking advantage of the high stability of *Sac*Pox, the supernatant was heated at 70°C during 30 minutes and centrifuged before proceeding a STREP-TRAP affinity chromatography step (GE Healthcare, Uppsala, Sweden). The sample was then cleaved by the Tobacco Etch Virus protease (TEV, ratio 1:20, w/w [56]) during 20 hours at 30°C prior to be loaded a second time on STREP-TRAP affinity chromatography. The flow through containing the cleaved protein was then concentrated and loaded on a size exclusion column (S75-16-60; GE Healthcare, Uppsala, Sweden). The protein purity and identity were checked by SDS-PAGE and mass spectrometry analysis (MS platform Timone, Marseille, France). The protein concentration was determined using a nanospectrophotometer (Nanodrop, Thermofisher Scientific, France) using its molar extinction coefficient (*Sac*Pox $\varepsilon_{280\ nm} = 35\ 307.7\ M^{-1}\ cm^{-1}$) calculated by the *PROT-PARAM* server [57].

Kinetic characterization

General procedures

Catalytic parameters were evaluated at 25°C and recorded with a microplate reader (Synergy HT, BioTek, USA) and the Gen5.1 software as previously explained [16,33,52,54]. The reaction was performed in a 200 μL volume using a 96-well plate with a 6.2 mm path length as previously described [33]. The collected data were subsequently fitted to the Michaelis-Menten (MM) equation [58] using *Graph-Pad Prism 5.00* (GraphPad Software, San Diego California USA, www.graphpad.com). In cases where V_{max} could not be reached, the catalytic efficiency was obtained by fitting the linear part of MM plot to a linear regression using *Graph-Pad Prism 5.00* software.

OP hydrolase and esterase kinetics

Standard assays for organophosphates (Figure 1A) and esters (Figure 1B) were performed in *activity buffer* (50 mM HEPES pH 8, 150 mM NaCl, 0.2 mM $CoCl_2$) by measuring the *p*-nitrophenolate release over time at 405 nm ($\varepsilon_{405\ nm} = 17\ 000\ M^{-1}\ cm^{-1}$). For ethyl-paraoxon (Additional file 1: Figure S1I), the *activity buffer* has also been supplemented with SDS (w/v) at 0.01% or 0.1% for detergent essays. Malathion (Additional file 1: Figure S1V) hydrolysis was followed at 412 nm in *activity buffer* added of 2 mM DTNB to follow the release of free thiols ($\varepsilon_{412\ nm} = 13\ 700\ M^{-1}\ cm^{-1}$). The time course hydrolysis of dihydrocoumarin (Additional file 1: Figure S1X), CMP-coumarin (Additional file 1: Figure S1VI) and phenylacetate (Additional file 1: Figure S1VII) were respectively monitored at 270 nm ($\varepsilon_{270\ nm} = 1\ 400\ M^{-1}\ cm^{-1}$), 412 nm ($\varepsilon_{412\ nm} = 37\ 000\ M^{-1}\ cm^{-1}$) and 270 nm ($\varepsilon_{270\ nm} = 1\ 400\ M^{-1}\ cm^{-1}$).

Lactonase kinetics

Kinetics monitoring the lactone hydrolysis were performed according to a previously described protocol [33]. The lactone hydrolysis was monitored in the *lactonase buffer* (2.5 mM Bicine pH 8.3, 150 mM NaCl, 0.2 mM $CoCl_2$, 0.25 mM Cresol purple and 0.5% DMSO) with different AHLs (Figure 1C) [*i.e.* C4-AHL (*r*), C6-AHL (*r*), C8-AHL (*r*), 3-oxo-C8-AHL (*l*), 3-oxo-C10-AHL (*l*)] (Additional file 1: Figure S1XI-XVI) and oxo-lactones (Figure 1D,E) [*i.e.* ε-caprolactone, γ-heptanolide (*r*), Nonanoic-γ-lactone (*r*), Nonanoic-δ-lactone (*r*), Undecanoic-γ-lactone (*r*), Undecanoic-δ-

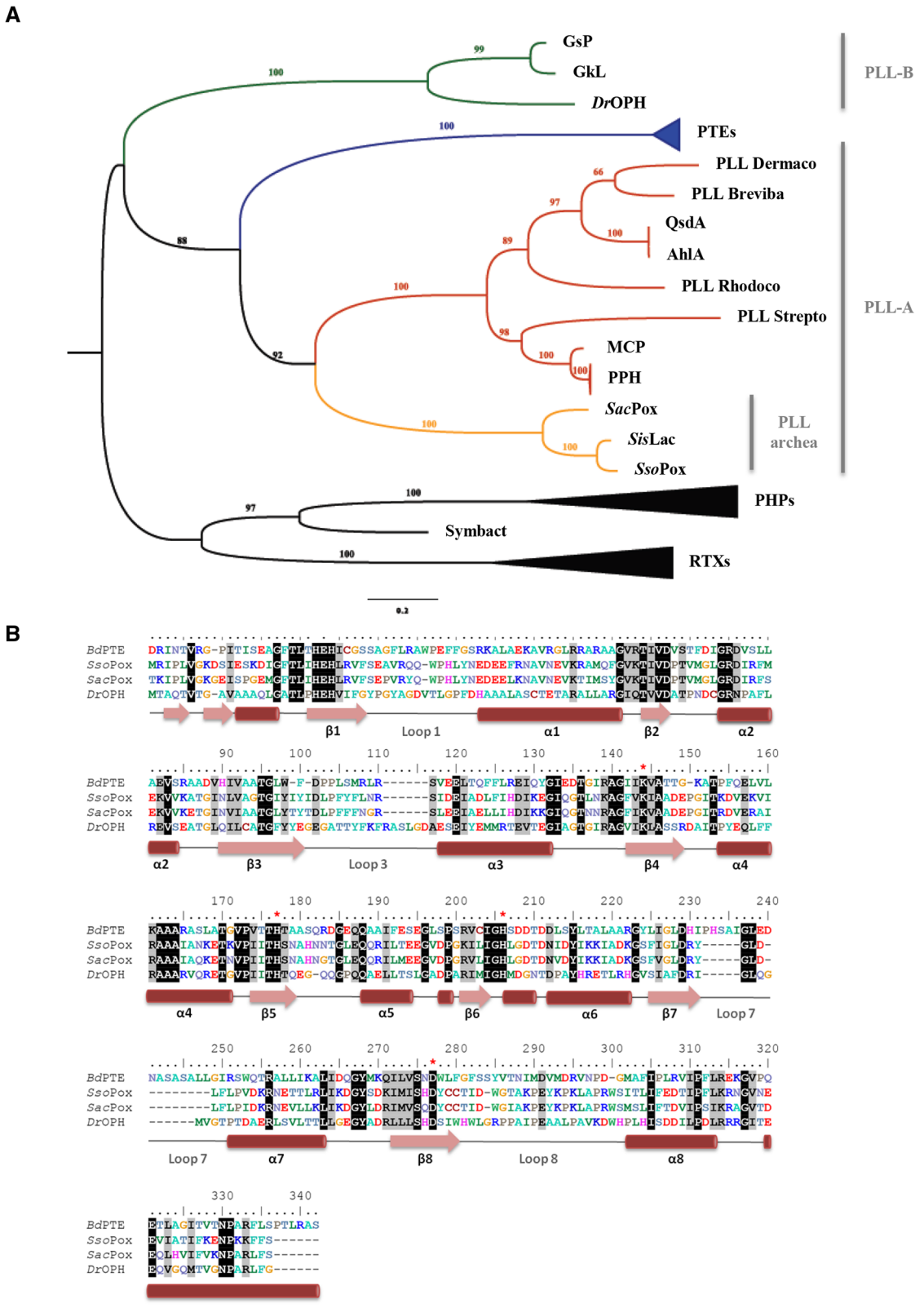

Figure 2 (See legend on next page.)

(See figure on previous page.)
Figure 2 Phylogenetic analysis of the PLL family. A. Phylogenetic tree of PLLs, PTEs, and close homologues. Members of PLL-B are colored in green while within the PLL-As, mesophilic and archaeal PLLs are respectively colored in red and orange. The clades of PHPs, PTEs and RTXs were collapsed for clarity. All the sequences used for this tree are listed in Additional file 1: Table S1. **B**. Sequence alignment of *Bd*PTE from *B. diminuta*, *Sso*Pox from *S. solfataricus*, *Sac*Pox from *S. acidocaldarius* and *Dr*OPH from *D. radiodurans*. Conserved amino acid residues are highlighted in black and similar residues in grey. Conserved active site residues involved in metals coordination are highlighted by red stars. Secondary structures are represented according to *Sso*Pox structure (with pink arrows depicting β-sheets and red cylinders depicting α-helixes).

lactone (*r*), Dodecanoic-γ-lactone (*r*) and Dodecanoic-δ-lactone (*r*)] (Additional file 1: Figure S1XVII-XXIV). Cresol purple (pK_a 8.3 at 25°C) is a pH indicator (577 nm) used to monitor the acidification of the medium following lactone ring hydrolysis ($\varepsilon_{577nm} = 5\,500\ M^{-1}\ cm^{-1}$).

Structural modeling and structural analysis

The *Sac*Pox structure was modelled using the *ESyPred3D* server using *Sac*Pox protein sequence as query and *Sso*Pox structure (2VC5) as template [59]. Structures were analyzed and figure made using PyMol [60].

Results

First classified within the bacterial PTEs, *Sac*Pox shares in fact only 33.8% sequence identity with *Bd*PTE (Additional file 1: Table S2). *Sac*Pox indeed belongs to the PLLs-A (Figure 2A) [2]: it shares 76.1% of sequence identity with its closest homologues *Sso*Pox and *Sis*Lac, and only 30.6% identity with the PLL-B *Dr*OPH. Together with *Sis*Lac and *Sso*Pox, *Sac*Pox comprises the creanarcheal clade of the PLLs-A (Figure 2A). The sequence alignment highlights the strict conservation of essential active site residues between the different clades (Figure 2B).

Enzymatic characterization

Phosphotriesterase activity

*Sac*Pox ability to hydrolyze insecticides ethyl/methyl-paraoxon, ethyl/methyl-parathion and malathion has been evaluated (Table 1). The best *Sac*Pox phosphotriester substrate, methyl-paraoxon is processed with moderate catalytic efficiency ($k_{cat}/K_M = 1.10(\pm0.17)\times10^3\ M^{-1}.s^{-1}$), low rate ($k_{cat} = 0.307\ s^{-1}$) and low K_M (278.3 μM). Very similar catalytic efficiencies were recorded for *Sso*Pox and *Sis*Lac: k_{cat}/K_M of $1.27\times10^3\ M^{-1}.s^{-1}$ and $4.26\times10^3\ M^{-1}.s^{-1}$, respectively [33,52]. Ethyl-paraoxon comprise a slower substrate, ($k_{cat}/K_M = 2.81\times10^2\ M^{-1}.s^{-1}$), highlighting the enzyme preference for OP substrates with small substituents. No hydrolysis could be measured for ethyl-parathion and malathion, whereas a low catalytic efficiency was recorded for methyl-parathion ($k_{cat}/K_M = 4.31\ M^{-1}.s^{-1}$). This specificity profile illustrates the clear preference of *Sac*Pox for oxono-phosphotriesters rather than thiono-phosphotriesters; as previously observed for *Sso*Pox [52] and *Sis*Lac [33]. Moreover, whereas anionic detergents like SDS can significantly stimulate *Sso*Pox phosphotriesterase activity [52], the same treatment on *Sac*Pox yields only a 2-fold increase in catalytic efficiency with ethyl-paraoxon as substrate. Finally, we show that *Sac*Pox hydrolyzes CMP-coumarin ($k_{cat}/K_M = 4.38\times10^2\ M^{-1}.s^{-1}$), albeit with 20-fold lower catalytic efficiency than *Sso*Pox [52].

Table 1 Phosphotriesterase kinetic parameters

	k_{cat} (s^{-1})	K_M (μM)	k_{cat}/K_M ($M^{-1}.s^{-1}$)
Paraoxon	0.12 ± 0.01	434 ± 54	2.81 (±0.38) × 10^2
Paraoxon 0.01% SDS	0.28 ± 0.01	537 ± 48	5.22 (±0.51) × 10^2
Paraoxon 0.1% SDS	0.25 ± 0.01	405 ± 21	6.10 (±0.34) × 10^2
Methyl Paraoxon	0.31 ± 0.02	278 ± 40	1.10 (±0.17) × 10^3
Parathion	ND	ND	ND
Methyl Parathion	ND	ND	4.31 ± 0.20
Malathion	ND	ND	ND
CMP-Coumarin	0.28 ± 0.02	642 ± 89	4.38 (±0.68) × 10^2

ND correspond to Not Detected hydrolysis. Results have been obtained with cobalt as cofactor.

Esterase activity

The ability of *Sac*Pox to hydrolyze phenyl-acetate, *p*NP-acetate and *p*NP-decanoate (Additional file 1: Figure S1VII-IX) has been evaluated (Table 2). While no activity could be detected against *p*NP-decanoate, *Sac*Pox exhibits low catalytic efficiencies against both phenyl-acetate and *p*NP-acetate ($k_{cat}/K_M \approx 50\ M^{-1}.s^{-1}$). This weak activity against classical esters differs from previous studies on the close homologues *Sso*Pox and *Sis*Lac, for which activity has only been recorded on *p*NP-acetate [33].

Lactonase activity

The catalytic parameters of *Sac*Pox for various lactone substrates have been measured, including against oxo-lactones (lipophilic aroma), AHLs and dihydrocoumarin (Table 3). Our results indicate a preference of *Sac*Pox for oxo-lactone substrates; *i.e.* γ-heptanolide and nonanoic-γ-lactone ($k_{cat}/K_M \approx 2.5\times10^4\ M^{-1}.s^{-1}$), while AHLs are about 10 times worse substrates (*i.e.*; C8 AHLs, $k_{cat}/K_M \approx 5\times10^3\ M^{-1}.s^{-1}$). Furthermore, it seems that *Sac*Pox prefers AHLs *vs* 3-oxo-AHLs since the K_M for C8 aliphatic chains is 5-fold lower than that for 3-oxo-C8 AHLs. Overall, long aliphatic chain substrates AHLs are better substrates for the enzyme. Indeed, short aliphatic chain AHLs are not hydrolyzed by *Sac*Pox. Interestingly, this preference is not retained for oxo-lactones, for which molecules with short

Table 2 Esterase kinetic parameters

	k_{cat} (s^{-1})	K_M (μM)	k_{cat}/K_M ($M^{-1}.s^{-1}$)
Phenyl-acetate	0.35 ± 0.05	8 181 ± 1750	42.3 ± 11.1
***p*NP-acetate**	0.13 ± 0.01	2 107 ± 313	60.1 ± 9.9
***p*NP-decanoate**	ND	ND	ND

ND correspond to Not Detected hydrolysis. Results have been obtained with cobalt as cofactor.

or without aliphatic chain are efficiently hydrolyzed ($k_{cat}/K_M \approx 10^4$ $M^{-1}.s^{-1}$). As previously observed for *Sso*Pox and *Sis*Lac [16,33], this feature may reveal a potential alternative binding mode of these compounds in *Sac*Pox active site. Finally, contrary to *Sso*Pox and *Sis*Lac [16,33], *Sac*Pox does not hydrolyze dihydrocoumarin.

Structural analysis

Numerous attempts to crystallize *Sac*Pox were made, with no success (Elias, Hiblot, Gotthard & Chabriere, unpublished). A previous structural model was generated by homology modeling based on *Bd*PTE structure [4] (~33.8% sequence identity with *Sac*Pox), but yielded little insights given the moderate sequence identity with the template and the very significant differences in the active site loops between these two representatives of distinct enzyme families [1,9,16]. Here we generated a homology-based model using the structure of *Sso*Pox as template (76.1% of sequence identity; Additional file 1: Table S2).

As expected, the *Sac*Pox model structure almost perfectly superimposes to the *Sso*Pox crystal structure (Figure 3A). Residues forming the active site are all conserved and residues involved in loops 7 and 8 occupy nearly identical conformation in *Sac*Pox and *Sso*Pox but also in *Sis*Lac structures (Figure 3B). Noteworthy, loop 8 is partially structured into an α-helix, as seen in X-ray structures of *Sso*Pox and *Sis*Lac. A substitution (I266 in *Sac*Pox; T265 in *Sso*Pox and *Sis*Lac) in loop 8 may slightly alter the shape of the aliphatic channel. But overall, the active site of *Sac*Pox and *Sso*Pox are nearly identical (Figure 2B). Furthermore, four other substitutions between *Sac*Pox and its close homologues can be seen in loop 8: *Sac*Pox exhibits a K at position 268, instead of an R residue (R267 in *Sis*Lac), Y271 instead of L (L270 in *Sis*Lac), K278 instead of R (R277 in both *Sis*Lac and *Sso*Pox), and M281 instead of I (I280 in *Sso*Pox) (Additional file 1: Figure S2). While the structural model suggests that these substitutions are not affecting directly the binding cleft of *Sac*Pox, they might modulate loop 8 conformation and its dynamics. Indeed, it was shown in the close homologue *Sso*Pox that a single substitution in loop 8 (W263 in *Sso*Pox, equivalent to W264 in *Sac*Pox) increases the conformational flexibility of loop 8, thereby conferring higher promiscuity to the enzyme [16]. The effect is in fact so dramatic that the substitution in *Sso*Pox of W263 by any of the 19 other natural amino acids yields a variant with improved phosphotriesterase activity [16]. Additionally, loop 8 being involved in the accommodation of the aliphatic substituent of lactones substrates [9], mutations in this loop can also affect the lactonase activity [16].

Table 3 Lactonase kinetic parameters

	k_{cat} (s^{-1})	K_M (μM)	k_{cat}/K_M ($M^{-1}.s^{-1}$)
C4 AHL	ND	ND	ND
C6 AHL	ND	ND	ND
C8 AHL	0.94 ± 0.02	178 ± 26	5.28 (±0.77) × 10^3
3-oxo C6 AHL	ND	ND	ND
3-oxo C8 AHL	0.89 ± 0.07	836 ± 178	1.07 (±0.25) × 10^3
3-oxo C10 AHL	1.03 ± 0.04	213 ± 33	4.88 (±0.77) × 10^3
γ heptanolide	10.25 ± 0.50	388 ± 62	2.64 (±0.44) × 10^4
Nonanoic-γ-lactone	2.64 ± 0.07	109 ± 19	2.44 (±0.44) × 10^4
Undecanoic-γ-lactone	0.34 ± 0.01	578 ± 78	5.89 (±0.84) × 10^2
dodecanoic-γ-lactone	0.53 ± 0.03	242 ± 60	2.21 (±0.57) × 10^3
Nonanoic-δ-lactone	4.55 ± 0.21	348 ± 53	1.31 (±0.21) × 10^4
Undecanoic-δ-lactone	1.05 ± 0.05	168 ± 37	6.22 (±1.40) × 10^3
Dodecanoic-δ-lactone	3.34 ± 0.07	185 ± 27	1.81 (±0.27) × 10^4
ε caprolactone	15.04 ± 0.47	1 031 ± 83	1.46 (±0.13) × 10^4
Dihydrocoumarine	ND	ND	ND

ND correspond to Not Detected hydrolysis. Results have been obtained with cobalt as cofactor.

Discussion

Here we show that *Sac*Pox is a proficient lactonase (~10^4 $M^{-1}.s^{-1}$) and can hydrolyze both oxo-lactones and AHLs. Nevertheless, *Sac*Pox have a slightly different substrate specificity than its close homologues [16,33]. Indeed, *Sac*Pox exhibits slightly lower catalytic efficiencies, prefers AHLs over 3-oxo-AHLs and does not show any activity against dihydrocoumarin. Interestingly, as noted for *Sis*Lac and *Sso*Pox [16,33], *Sac*Pox clearly prefers long chain AHLs, but can efficiently hydrolyze short chain or oxo-lactones without aliphatic substituents. This feature could reflect a putatively different binding mode of AHLs and oxo-lactones into PLLs active sites. We note that the biological role of lactonases such as PLLs is yet unclear, especially in extremophilic archaea where no AHL-based *quorum* sensing systems have been identified so far.

*Sac*Pox also exhibits promiscuous esterase and phosphotriesterase activities, a common feature of PLLs. Similarly to *Sso*Pox and *Sis*Lac [33,52], *Sac*Pox prefers OPs with small substituents. Moreover, *Sac*Pox also shows a clear preference for oxono-phosphotriesters, rather than thiono-phosphotriesters, a feature previously dubbed thiono-effect [52]. Interestingly, *Sso*Pox, *Sis*Lac and *Sac*Pox exhibit similar catalytic efficiencies against OPs (10^{2-3} $M^{-1}.s^{-1}$) at 25°C, efficiencies that are close to those measured at much higher temperatures [4].

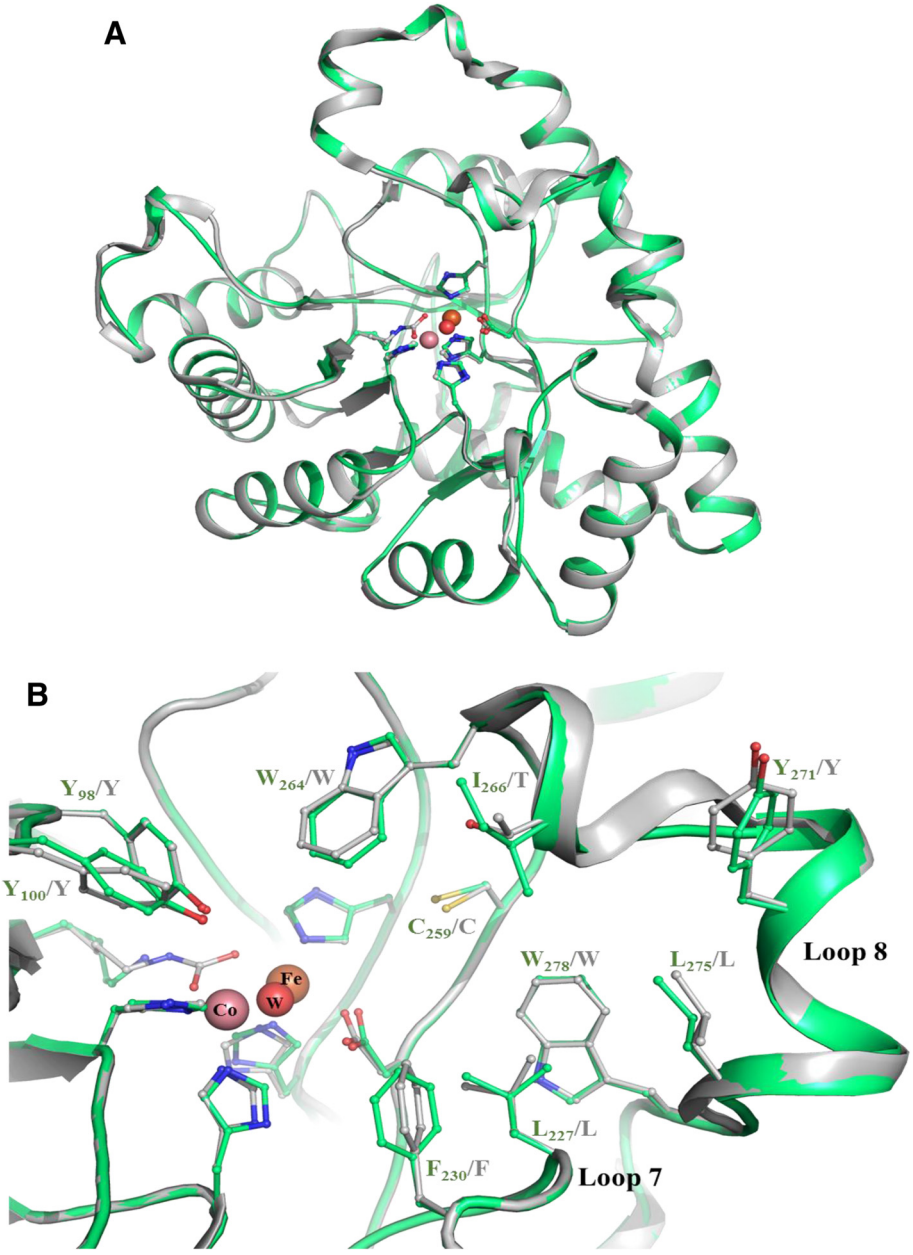

Figure 3 Structural model of *Sac*Pox. A. Structural superposition of *Sso*Pox structure (2VC5; grey) and the *Sac*Pox model (green). Cobalt, iron and the catalytic water molecule are respectively represented by pink, orange and red spheres. Bimetallic center coordinating residues are represented as sticks. **B**. Active site view of superimposed *Sso*Pox structure (grey) and the *Sac*Pox model (green). Several active site residues are represented as sticks. Numbering is made according to *Sac*Pox sequence.

The structural model shows that *Sac*Pox structure is very close to that of *Sso*Pox (Figure 2A). Most critically, the active sites of both enzymes are essentially identical (Figure 2B), with the exception of position 266 (I in *Sac*Pox, T in *Sso*Pox and *Sis*Lac). This substitution might partly account for the observed differences in substrates specificity between these enzymes, and would thereby represent an interesting target for future mutagenesis studies. But four other substitutions in loop 8 between these close homologues might be involved as well, and comprise also interesting options for mutagenesis studies (K268R, Y27IL, K278R and M281I). A recent study on *Sso*Pox highlighted how profound the effect on catalysis of a single substitution on loop 8 (W263) can be [16]. Therefore, substitution T266I, and/or the four others on loop 8, might contribute to the observed differences between *Sac*Pox and *Sso*Pox in substrate specificity, in combination with other factors that cannot be assessed

by a structural model such as subtle changes in active site loops conformation and dynamics [16,33]. Indeed, the observed differences in the detergent stimulation between both enzymes (*Sac*Pox is only weakly stimulated by SDS, as compared to *Sso*Pox) could well be a manifestation of different dynamics of their respective active site loops.

Conclusions

To conclude, we here demonstrate that albeit being initially isolated, characterized, and named after its ability to degrade the insecticide paraoxon (pox; [4]), *Sac*Pox is putatively a native lactonase, capable of hydrolyzing these compounds with significant catalytic efficiencies at 25°C (up to 10^4 $M^{-1}.s^{-1}$). The extensive kinetic characterization reveals some substrate specificity differences between *Sac*Pox and its close homologues *Sis*Lac and *Sso*Pox, and the proposed structural model of *Sac*Pox suggests putative candidates (*e.g.* I266) that could account for these observations. Such positions might constitute interesting targets for future engineering studies, with the aim of improving or altering the catalytic properties of *Sac*Pox.

Additional file

Additional file 1: Figure S1. Chemical structure of phosphoesters (I-VI), esters (VII-IX) and lactones (X-XXIV). **Figure S2.** Superposition of *Sso*Pox, *Sis*Lac and *Sac*Pox structural models. **Table S1.** Accession numbers of the sequences used in the phylogeny study. **Table S2.** Sequence identity matrix.

Competing interests

The authors declare that they have no competing interests.

Authors' contributions

JH, GG and ME planed the experiments. JB, CC performed the experiments. JH, JB, ME and EC analysed the results. JB, JH and ME wrote the paper. All the authors offered a critical review of the paper.

Acknowledgements

We are grateful to Dr. Moshe Goldsmith for the kind gift of CMP-coumarin. This work was granted by DGA, France (REI. 2009 34 0045). J.B. is a PhD student granted by DGA. J.H. and C.C. are founded by DGA, France. G.G. is founded by APHM, France.

Received: 4 February 2014 Accepted: 27 May 2014
Published: 3 June 2014

References

1. Afriat L, Roodveldt C, Manco G, Tawfik DS: **The latent promiscuity of newly identified microbial lactonases is linked to a recently diverged phosphotriesterase.** *Biochemistry* 2006, **45:**13677–13686.
2. Afriat-Jurnou L, Jackson CJ, Tawfik DS: **Reconstructing a missing link in the evolution of a recently diverged phosphotriesterase by active-site loop remodeling.** *Biochemistry* 2012, **51:**6047–6055.
3. Merone L, Mandrich L, Rossi M, Manco G: **A thermostable phosphotriesterase from the archaeon Sulfolobus solfataricus: cloning, overexpression and properties.** *Extremophiles* 2005, **9:**297–305.
4. Porzio E, Merone L, Mandrich L, Rossi M, Manco G: **A new phosphotriesterase from Sulfolobus acidocaldarius and its comparison with the homologue from Sulfolobus solfataricus.** *Biochimie* 2007, **89:**625–636.
5. Xiang DF, Kolb P, Fedorov AA, Meier MM, Fedorov LV, Nguyen TT, Sterner R, Almo SC, Shoichet BK, Raushel FM: **Functional annotation and three-dimensional structure of Dr0930 from Deinococcus radiodurans, a close relative of phosphotriesterase in the amidohydrolase superfamily.** *Biochemistry* 2009, **48:**2237–2247.
6. Hawwa R, Larsen SD, Ratia K, Mesecar AD: **Structure-based and random mutagenesis approaches increase the organophosphate-degrading activity of a phosphotriesterase homologue from Deinococcus radiodurans.** *J Mol Biol* 2009, **393:**36–57.
7. Dumas DP, Caldwell SR, Wild JR, Raushel FM: **Purification and properties of the phosphotriesterase from Pseudomonas diminuta.** *J Biol Chem* 1989, **264:**19659–19665.
8. Singh BK: **Organophosphorus-degrading bacteria: ecology and industrial applications.** *Nat Rev Microbiol* 2009, **7:**156–164.
9. Elias M, Dupuy J, Merone L, Mandrich L, Porzio E, Moniot S, Rochu D, Lecomte C, Rossi M, Masson P, Manco G, Chabriere E: **Structural basis for natural lactonase and promiscuous phosphotriesterase activities.** *J Mol Biol* 2008, **379:**1017–1028.
10. Benning MM, Kuo JM, Raushel FM, Holden HM: **Three-dimensional structure of phosphotriesterase: an enzyme capable of detoxifying organophosphate nerve agents.** *Biochemistry* 1994, **33:**15001–15007.
11. Seibert CM, Raushel FM: **Structural and catalytic diversity within the amidohydrolase superfamily.** *Biochemistry* 2005, **44:**6383–6391.
12. Roodveldt C, Tawfik DS: **Shared promiscuous activities and evolutionary features in various members of the amidohydrolase superfamily.** *Biochemistry* 2005, **44:**12728–12736.
13. Porzio E, Di Gennaro S, Palma A, Manco G: **Mn(2+) modulates the kinetic properties of an archaeal member of the PLL family.** *Chem Biol Interact* 2013, **203:**251–256.
14. Xue B, Chow JY, Baldansuren A, Yap LL, Gan YH, Dikanov SA, Robinson RC, Yew WS: **Correction to structural evidence of a productive active site architecture for an evolved quorum-quenching GKL lactonase.** *Biochemistry* 2012, **51:**10120.
15. Bigley AN, Raushel FM: **Catalytic mechanisms for phosphotriesterases.** *Biochim Biophys Acta* 2013, **1834:**443–453.
16. Hiblot J, Gotthard G, Elias M, Chabriere E: **Differential active site loop conformations mediate promiscuous activities in the lactonase pox.** *PLoS One* 2013, **8:**e75272.
17. Waters CM, Bassler BL: **Quorum sensing: cell-to-cell communication in bacteria.** *Annu Rev Cell Dev Biol* 2005, **21:**319–346.
18. Popat R, Crusz SA, Diggle SP: **The social behaviours of bacterial pathogens.** *Br Med Bull* 2008, **87:**63–75.
19. Boyen F, Eeckhaut V, Van Immerseel F, Pasmans F, Ducatelle R, Haesebrouck F: **Quorum sensing in veterinary pathogens: mechanisms, clinical importance and future perspectives.** *Vet Microbiol* 2009, **135:**187–195.
20. Elias M, Tawfik DS: **Divergence and convergence in enzyme evolution: parallel evolution of paraoxonases from quorum-quenching lactonases.** *J Biol Chem* 2012, **287:**11–20.
21. Amara N, Krom BP, Kaufmann GF, Meijler MM: **Macromolecular inhibition of quorum sensing: enzymes, antibodies, and beyond.** *Chem Rev* 2011, **111:**195–208.
22. Hentzer M, Wu H, Andersen JB, Riedel K, Rasmussen TB, Bagge N, Kumar N, Schembri MA, Song Z, Kristoffersen P, Manefield M, Costerton JW, Molin S, Eberl L, Steinberg P, Kjelleberg S, Høiby N, Givskov M: **Attenuation of Pseudomonas aeruginosa virulence by quorum sensing inhibitors.** *EMBO J* 2003, **22:**3803–3815.
23. O'Loughlin CT, Miller LC, Siryaporn A, Drescher K, Semmelhack MF, Bassler BL: **A quorum-sensing inhibitor blocks Pseudomonas aeruginosa virulence and biofilm formation.** *Proc Natl Acad Sci U S A* 2013, **110:**17981–17986.
24. Wu H, Song Z, Hentzer M, Andersen JB, Molin S, Givskov M, Hoiby N: **Synthetic furanones inhibit quorum-sensing and enhance bacterial clearance in Pseudomonas aeruginosa lung infection in mice.** *J Antimicrob Chemother* 2004, **53:**1054–1061.
25. Christensen LD, van Gennip M, Jakobsen TH, Alhede M, Hougen HP, Hoiby N, Bjarnsholt T, Givskov M: **Synergistic antibacterial efficacy of early combination treatment with tobramycin and quorum-sensing inhibitors against Pseudomonas aeruginosa in an intraperitoneal foreign-body infection mouse model.** *J Antimicrob Chemother* 2012, **67:**1198–1206.
26. Dong YH, Wang LH, Xu JL, Zhang HB, Zhang XF, Zhang LH: **Quenching quorum-sensing-dependent bacterial infection by an N-acyl homoserine lactonase.** *Nature* 2001, **411:**813–817.
27. Dong YH, Wang LY, Zhang LH: **Quorum-quenching microbial infections: mechanisms and implications.** *Philos Trans R Soc Lond B Biol Sci* 2007, **362:**1201–1211.

28. Ng FS, Wright DM, Seah SY: **Characterization of a phosphotriesterase-like lactonase from Sulfolobus solfataricus and its immobilization for quorum quenching.** *Appl Environ Microbiol* 2011, **77:**1181–1186.
29. Krieger RI: *Handbook of Pesticide Toxicology.* 2nd edition. San Diego: Academic Press; 2001.
30. Gupta RC: *Handbook of Toxicology of Chemical Warfare Agents.* San Diego: Elsevier Inc; 2009.
31. LeJeune KE, Wild JR, Russell AJ: **Nerve agents degraded by enzymatic foams.** *Nature* 1998, **395:**27–28.
32. Hawwa R, Aikens J, Turner RJ, Santarsiero BD, Mesecar AD: **Structural basis for thermostability revealed through the identification and characterization of a highly thermostable phosphotriesterase-like lactonase from Geobacillus stearothermophilus.** *Arch Biochem Biophys* 2009, **488:**109–120.
33. Hiblot J, Gotthard G, Chabriere E, Elias M: **Structural and enzymatic characterization of the lactonase SisLac from Sulfolobus islandicus.** *PLoS One* 2012, **7:**e47028.
34. Hiblot J, Gotthard G, Champion C, Chabriere E, Elias M: **Crystallization and preliminary X-ray diffraction analysis of the lactonase VmoLac from Vulcanisaeta moutnovskia.** *Acta Crystallogr Sect F Struct Biol Cryst Commun* 2013, **69:**1235–1238.
35. Vieille C, Zeikus GJ: **Hyperthermophilic enzymes: sources, uses, and molecular mechanisms for thermostability.** *Microbiol Mol Biol Rev* 2001, **65:**1–43.
36. Demirjian DC, Moris-Varas F, Cassidy CS: **Enzymes from extremophiles.** *Curr Opin Chem Biol* 2001, **5:**144–151.
37. Burton SG, Cowan DA, Woodley JM: **The search for the ideal biocatalyst.** *Nat Biotechnol* 2002, **20:**37–45.
38. Singh RK, Tiwari MK, Singh R, Lee JK: **From protein engineering to immobilization: promising strategies for the upgrade of industrial enzymes.** *Int J Mol Sci* 2013, **14:**1232–1277.
39. Merone L, Mandrich L, Porzio E, Rossi M, Muller S, Reiter G, Worek F, Manco G: **Improving the promiscuous nerve agent hydrolase activity of a thermostable archaeal lactonase.** *Bioresour Technol* 2010, **101:**9204–9212.
40. Meier MM, Rajendran C, Malisi C, Fox NG, Xu C, Schlee S, Barondeau DP, Hocker B, Sterner R, Raushel FM: **Molecular engineering of organophosphate hydrolysis activity from a weak promiscuous lactonase template.** *J Am Chem Soc* 2013, **135:**11670–11677.
41. Zhang Y, An J, Ye W, Yang G, Qian ZG, Chen HF, Cui L, Feng Y: **Enhancing the promiscuous phosphotriesterase activity of a thermostable lactonase (GkaP) for the efficient degradation of organophosphate pesticides.** *Appl Environ Microbiol* 2012, **78:**6647–6655.
42. Chow JY, Wu L, Yew WS: **Directed evolution of a quorum-quenching lactonase from Mycobacterium avium subsp. paratuberculosis K-10 in the amidohydrolase superfamily.** *Biochemistry* 2009, **48:**4344–4353.
43. Chow JY, Xue B, Lee KH, Tung A, Wu L, Robinson RC, Yew WS: **Directed evolution of a thermostable quorum-quenching lactonase from the amidohydrolase superfamily.** *J Biol Chem* 2010, **285:**40911–40920.
44. Auernik KS, Cooper CR, Kelly RM: **Life in hot acid: pathway analyses in extremely thermoacidophilic archaea.** *Curr Opin Biotechnol* 2008, **19:**445–453.
45. Gotthard G, Hiblot J, Elias M, Chabriere E: **Crystallization and preliminary X-ray diffraction analysis of the hyperthermophilic Sulfolobus islandicus lactonase.** *Acta Crystallogr Sect F Struct Biol Cryst Commun* 2011, **67:**354–357.
46. Del Vecchio P, Elias M, Merone L, Graziano G, Dupuy J, Mandrich L, Carullo P, Fournier B, Rochu D, Rossi M, Masson P, Chabriere E, Manco G: **Structural determinants of the high thermal stability of SsoPox from the hyperthermophilic archaeon Sulfolobus solfataricus.** *Extremophiles* 2009, **13:**461–470.
47. Notredame C, Higgins DG, Heringa J: **T-Coffee: a novel method for fast and accurate multiple sequence alignment.** *J Mol Biol* 2000, **302:**205–217.
48. Poirot O, O'Toole E, Notredame C: **Tcoffee@igs: a web server for computing, evaluating and combining multiple sequence alignments.** *Nucleic Acids Res* 2003, **31:**3503–3506.
49. Gouy M, Guindon S, Gascuel O: **SeaView version 4: a multiplatform graphical user interface for sequence alignment and phylogenetic tree building.** *Mol Biol Evol* 2010, **27:**221–224.
50. Hall TA: **BioEdit: a user-friendly biological sequence alignment editor and analysis program for Windows 95/98/NT.** *Nucleic Acids Symposium Series* 1999, **41:**95–98.
51. Larkin MA, Blackshields G, Brown NP, Chenna R, McGettigan PA, McWilliam H, Valentin F, Wallace IM, Wilm A, Lopez R, Thompson JD, Gibson TJ, Higgins DG: **Clustal W and Clustal X version 2.0.** *Bioinformatics* 2007, **23:**2947–2948.
52. Hiblot J, Gotthard G, Chabriere E, Elias M: **Characterisation of the organophosphate hydrolase catalytic activity of SsoPox.** *Sci Rep* 2012, **2:**779.
53. Gotthard G, Hiblot J, Gonzalez D, Chabriere E, Elias M: **Crystallization and preliminary X-ray diffraction analysis of the organophosphorus hydrolase OPHC2 from Pseudomonas pseudoalcaligenes.** *Acta Crystallogr Sect F Struct Biol Cryst Commun* 2013, **69:**73–76.
54. Gotthard G, Hiblot J, Gonzalez D, Elias M, Chabriere E: **Structural and enzymatic characterization of the phosphotriesterase OPHC2 from Pseudomonas pseudoalcaligenes.** *PLoS One* 2013, **8:**e77995.
55. Studier FW: **Protein production by auto-induction in high density shaking cultures.** *Protein Expr Purif* 2005, **41:**207–234.
56. van den Berg S, Lofdahl PA, Hard T, Berglund H: **Improved solubility of TEV protease by directed evolution.** *J Biotechnol* 2006, **121:**291–298.
57. Wilkins MR, Gasteiger E, Bairoch A, Sanchez JC, Williams KL, Appel RD, Hochstrasser DF: **Protein identification and analysis tools in the ExPASy server.** *Methods Mol Biol* 1999, **112:**531–552.
58. Copeland RA: *Enzymes, A Practical Introduction to Structure, Mechanism, and Data Analysis.* 2nd edition. New York, Chichester, Weiheim, Brisbane, Singapore, Toronto: WILEY-VCH; 2000.
59. Lambert C, Leonard N, De Bolle X, Depiereux E: **ESyPred3D: prediction of proteins 3D structures.** *Bioinformatics* 2002, **18:**1250–1256.
60. DeLano W: *The PyMOL Molecular Graphics System.* San Carlos, CA, USA: DeLano Scientific; 2002.

doi:10.1186/1756-0500-7-333
Cite this article as: Bzdrenga *et al.*: *Sac*Pox from the thermoacidophilic crenarchaeon *Sulfolobus acidocaldarius* is a proficient lactonase. *BMC Research Notes* 2014 **7**:333.